Experimental and theoretical studies of oxygen ordering in quenched and slow-cooled $YBa_2Cu_3O_{7-\delta}$

L. E. Levine and M. Däumling
IBM Research Division, Thomas J. Watson Research Center, Yorktown Heights, New York 10598
(Received 27 November 1991)

Two curves for T_c vs δ in $YBa_2Cu_3O_{7-\delta}$ are found in the literature; slow-cooled samples show 60 and 90 K plateaus while quenched specimens show a nearly linear decrease of T_c with increasing δ. We present a comprehensive electron-diffraction study of quenched specimens and show that there are pronounced differences in the oxygen ordering between quenched and slow-cooled samples. A simple model, in which the average antiphase domain size is the only adjustable parameter, is found to match all of the experimental electron-diffraction data to within measurement error.

Oxygen ordering in the Cu-O chains of $YBa_2Cu_3O_{7-\delta}$ is currently a topic of great interest.[1-12] These oxygen-vacancy structures and their effects on the superconducting parameters of $YBa_2Cu_3O_{7-\delta}$ are poorly understood, and a deeper insight into this topic could lead to a greater understanding of the basic mechanism of high-T_c superconductivity. Previous transmission electron microscopy (TEM) studies using selected area diffraction (SAD) have shown diffuse scattering features along the a^* direction.[1,7,9,11] The T_c versus δ behavior of the slow-cooled $YBa_2Cu_3O_{7-\delta}$ material used in these earlier studies displayed the characteristic plateaus frequently reported in the literature.[1,7,11,13] In this paper we present the results of TEM oxygen-ordering studies on quenched material possessing a nearly linear T_c dependence on δ. We find diffuse scattering features that are different from those observed in previous studies. An oxygen-ordering model is also presented that correctly describes all available diffuse scattering data from both quenched and slow-cooled $YBa_2Cu_3O_{7-\delta}$ for the oxygen deficiency range $0 \le \delta < 0.5$. The model has just one adjustable parameter: the average size of antiphase domains (APD) in the sample. Previous attempts to model the oxygen-vacancy structures responsible for these diffuse scattering features have primarily concentrated on low-energy-state oxygen configurations. We compare these model predictions with our experimental results.

Specimens were prepared using a liquid-phase processing method similar to that described by Salama *et al.*[14] Specific oxygen deficiencies were obtained by annealing the samples at a fixed temperature (600–660 °C) and oxygen partial pressure (either air or 1 atm of oxygen) for typically 24 h. Thermogravimetric measurements proved that this annealing time was sufficient to ensure uniform oxygenation to the equilibrium stoichiometry. The samples were then quenched by dropping them into an aluminum surface; the total quenching time for this process was less than 5 sec. Oxygen deficiencies were thus determined strictly by the annealing temperature and the oxygen partial pressure.[15] Samples were annealed at room temperature for at least one week prior to any measurements. As explained elsewhere,[16] neither our samples nor the slow-cooled samples of Beyers *et al.* were fully equilibrated.

The superconducting critical temperature T_c was determined using a standard two-coil low-frequency ac-susceptibility method which measures the diamagnetic shielding as a function of temperature. The midpoints of the transitions as a function of δ are shown in Fig. 1; the error bars signify 10% and 90% values for the shielding. Mechanical removal of a surface layer by grinding the specimen did not significantly alter the T_c. The observed variation of T_c with oxygen deficiency does not display the pronounced double-plateau structure found in slow-cooled samples but instead exhibits an approximately linear decrease with increasing oxygen deficiency. This linear behavior has previously been reported in sintered specimens.[17] The diamonds in Fig. 1 represent diamagnetic onset values from Beyers *et al.*;[1] Our onsets occurred at significantly lower temperatures.

Following the sample-preparation procedure used by Beyers,[18] specimens were ground up in ethyl alcohol and placed, using a pipette, onto holey carbon grids for examination in a Phillips 430 TEM. This procedure minimized the possibility of altering the quenched-in oxygen ordering structures. Electron-beam energies of 100 kV were used since energies greater than 150 kV were found to have visible effects on the diffuse scattering features observed in the SAD patterns.

Specimens with oxygen deficiencies of $\delta = 0.43$, 0.38, 0.35, 0.32, 0.27, 0.18, and < 0.05 were examined using SAD primarily from (001) orientations. Eight to twenty grains of various thicknesses were examined for each stoichiometry. Samples ranged from nearly transparent to nearly opaque to the electron beam. The shapes of the diffuse scattering structures showed little variation with sample thickness. This suggests that kinematical calculations of diffuse scattering from theoretical oxygen-ordering configurations could be successfully compared with the data. Diffuse scattering intensity along the a^* axis formed slightly broadened Ortho II peaks at $a^*/2$ for $\delta = 0.43$; these peaks gradually broadened into centered streaks of length $\simeq 0.3a^*$ at $\delta = 0.32$. Specimens with $\delta = 0.27$ showed two distinct oxygen-ordering structures from different grains: a long centered streak similar to that observed in the $\delta = 0.32$ samples and a double-peak structure similar to those reported by Beyers *et al.*[1] The diffuse scattering from samples with $\delta = 0.18$ formed

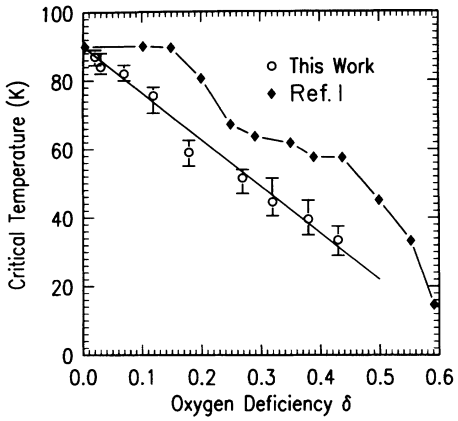

FIG. 1. Inductively measured superconducting transition temperatures T_c for $YBa_2Cu_3O_{7-\delta}$ as a function of oxygen deficiency δ. The diamonds represent diamagnetic onsets for slow-cooled samples and the circles represent the transition midpoints for quenched specimen. The error bars represent 10% and 90% values for the shielding.

extremely weak continuous streaks. This streaking was not observed in all samples. A fully oxygenated sample with $\delta < 0.05$ showed no diffuse scattering along a^*.

The streaks of diffuse scattering along the a^* direction were relatively very narrow for all oxygen deficiencies. We estimate that the average continuous oxygen chain domain sizes along the b axis must be at least 150 Å to produce these narrow features. The existence of such long oxygen chains along the b axis suggests that a one-dimensional oxygen-ordering model similar to the Magneli phase model proposed by Khachaturyan *et al.*[2] may suffice for describing the observed electron diffraction results. The large extent of the features along the a^* axis indicates that oxygen-vacancy correlations along the a axis are primarily short range. SAD patterns from (100) and (010) orientations show broad c^* streaks, thus demonstrating significant disorder between a-b planes. Unfortunately, the oxygen-coherence lengths for the non-Ortho II structures were shorter than the sample thicknesses for all orientations, thus making high-resolution imaging useless for determining the oxygen-ordering structures directly.

The standard Ortho II structure ($\delta = 0.5$) on an a-b plane is composed of alternating occupied and vacant (010) oxygen chains with the vacancies occurring on the oxygen chain sites. Adding additional occupied chains can be accomplished either by filling in vacant chains in the Ortho II structure (forming fully oxygenated 3-chain structures) or by introducing 2-chain oxygen structures. Both configurations are shown in Fig. 2, where solid circles represent fully oxygenated unit cells and open circles represent cells with oxygen vacancies. Adding oxygen by introducing only 2-chain structures with no long-range correlations results in the Magneli-type defect model[2] of Khachaturyan *et al.*

The 2-chain and 3-chain oxygen structures described above have very different properties. Adding oxygens into Ortho II vacancy chains with no long-range correlations does not alter the basic Ortho II character of the diffuse scattering. As vacancy chains are randomly filled, the sharp peak at $a^*/2$ decreases in amplitude but remains sharp; additional scattering amplitude forms uniform streaks along a^*. Adding oxygen by introducing 2-chain structures, however, disrupts the basic character of the Ortho II configuration by creating antiphase boundaries (APB) with the Ortho II structures having opposite phases on both sides of the boundary. These APB's broaden the original Ortho II peak and eventually introduce peak splitting as the structure tends toward a repeated arrangement of double oxygen chains separated by single-vacancy chains. This structure results in sharp peaks at $a^*/3$ and $2a^*/3$ for the oxygen stoichiometry $YBa_2Cu_3O_{6.66}$. Although this 2-chain model[2] successfully predicts a double-peak structure similar to that observed in TEM data, the details of peak shape as a function of oxygen deficiency are incorrect; the model is also limited to the range $0.33 \leq \delta \leq 0.5$.

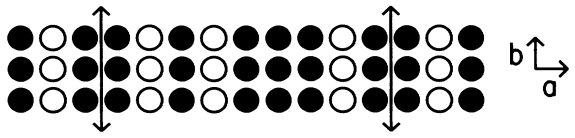

FIG. 2. Example $YBa_2Cu_3O_{7-\delta}$ oxygen-vacancy structure. The solid circles represent fully oxygenated unit cells and the open circles represent cells with oxygen vacancies. The vertical black lines delineate a single antiphase domain.

The above considerations suggest a model in which the average APD size is the critical parameter. Instead of assuming perfect Ortho II domains joined by APB's,[2] we introduced Ortho II defects by adding oxygens into normally vacant chains. This random filling does not break the double-period translational symmetry but does reduce the long-range-order parameter of the Ortho II domains. The number of defects is determined by the average APD size and the oxygen stoichiometry. This model therefore extends the earlier model of Khachaturyan *et al.* by allowing partially disordered Ortho II domains between APB's. Figure 2 shows a single APD delineated by vertical black lines. The 3-chain oxygen structure is not an APB since only even numbered chain structures form such boundaries. In our model we put in an average APD size and an oxygen stoichiometry. From this we calculate the probabilities for having double-oxygen chains breaking an Ortho II structure. The probability distribution is flat since we assume no long-range correlations. Additional oxygen chains are added by randomly filling in the remaining vacancy chains until the desired oxygen stoichiometry is reached. This model can produce oxygen structures in the deficiency range $0 \leq \delta \leq 0.5$. Oxygen deficiencies greater than 0.5 could have been obtained by introducing oxygen-vacancy defects into the Ortho II domains.

Using the above model we computer generated oxygen structures and calculated their Fourier transforms to simulate the experimental SAD patterns. Arbitrary scattering intensities were chosen for the occupied and vacant unit cells since this only affected the absolute in-

tensity of the diffuse scattering. Oxygen sequences of 1000 unit cells were found to be sufficient to reduce finite-size effects to below experimentally measurable limits. For each calculation, Fourier transforms from 5000 independent configurations were averaged to minimize noise in the final results. The oxygen deficiencies were determined from the sample stoichiometries leaving the APD size as the only adjustable parameter. Fits were attempted for all of our SAD data. In all cases, the model was found to fit the observed diffuse scattering features to within measurement error. For SAD patterns showing single peaks, fits were made to the widths and shapes of the peaks. Relative intensities were determined from SAD electron micrographs taken using a wide range of exposure times. For the SAD patterns showing double peaks, the fit was made to the measured peak-peak separation distance which could be measured very accurately. Theoretical diffuse scattering structures generated to match this peak separation were found to also match the observed peak widths and shapes to within measurement error.

Results of the calculations for four of our fits are shown in Fig. 3(a). Data points for the $\delta=0.27$ split-peak structure demonstrate the accuracy of the fit; the error bars are given by the symbol sizes. The fits were for data taken at oxygen deficiencies of 0.43, 0.35, and 0.27. The average APD sizes used to generate the fits to our data are given by open circles in Fig. 4. The error bars for these fits represent 1σ errors. The lowest point shows no error bars because the error was much smaller than the symbol size. This data point corresponds to the split-peak structure shown in Fig. 3(a). Figure 3(b) shows fits to data published by Beyers *et al.*[1] The corresponding average APD sizes are shown as solid diamonds in Fig. 4. The fits for the double-peak structures at $\delta=0.35$ and $\delta=0.29$ were made using the measured peak spacings of Beyers *et al.* The digitized data Beyers *et al.* provided for the single-peak structure at $\delta=0.35$ were also good enough to allow attempts at fitting. Although the absence of the original data made error estimates unreliable, the errors for the double-peaked data are probably very small since the reported peak separations were the only required input parameter. The reported peak separation for $\delta=0.25$ is suspect since the measured peak sits on a sloping background from the primary peaks. The error bars for this data point result from estimates of this uncertainty. The dashed line in Fig. 4 represents a lower limit for the model presented in this paper. APD sizes below this line would require adjacent oxygen vacancies to reach the necessary oxygen deficiency. The simulations of Khachaturyan *et al.* would fall on this line.

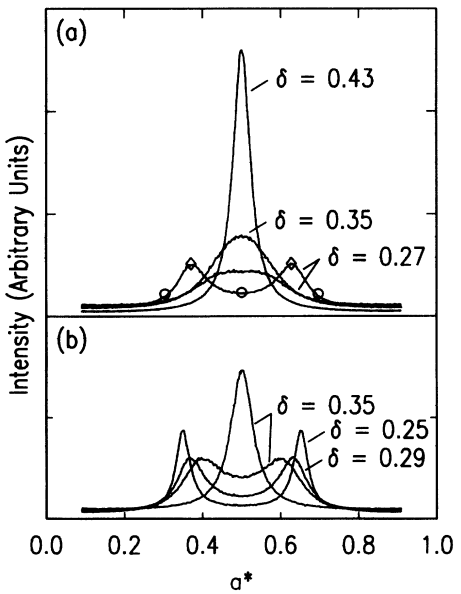

FIG. 3. Theoretical fits to experimental selected area diffraction data. Data is from (a) our quenched samples and from (b) slow-cooled samples of Beyers *et al.*

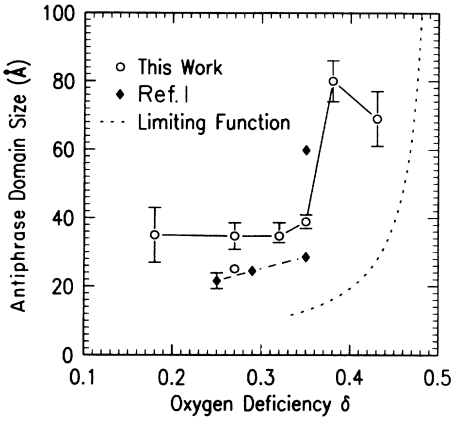

FIG. 4. Average antiphase domain sizes determined from theoretical fits to selected area diffraction data from our quenched samples and from slow-cooled samples of Beyers *et al.*

The oxygen-ordering structures in our quenched specimens are clearly different from the structures observed in the slow-cooled samples of Beyers *et al.* In Fig. 4, most of our data below $\delta=0.35$ have an average APD size of approximately 36 Å. All of the corresponding diffuse scattering features have a single central peak. Our remaining data point at $\delta=0.27$ and three of the slow-cooled sample data points have smaller APD sizes and exhibit double peaks. In our $\delta=0.27$ specimens we found no diffuse scattering structures intermediate between the two structures shown in Fig. 3(a), suggestive of a two-phase region. Beyers *et al.*[1] state that the presence of two distinct oxygen-ordering structures in their $\delta=0.35$ samples is consistent with the idea that the 60°-K plateau could be caused by phase separation of two ordered structures. Our data from quenched material shows no plateau and only one phase at $\delta=0.35$, thus supporting this hypothesis.

As shown in Fig. 1, samples produced by different cooling procedures exhibit different critical temperatures for the same oxygen deficiency. This suggests oxygen ordering as a likely cause for this difference. Our studies confirm this hypothesis by demonstrating and quantifying the oxygen-ordering differences between slow-cooled and

quenched samples. We conclude that, for a given oxygen stoichiometry, smaller APD's are favored at lower temperatures and result in higher T_c's. The next step is to relate the observed oxygen-ordering structures with the corresponding critical temperatures. We suggest that hole concentration calculations similar to those of Zaanen *et al.*[19] could be used with our predicted oxygen-ordering structures to produce a more accurate picture of the T_c dependence on in-plane hole concentrations.

The APB's discussed above can also be thought of as very small domains of Ortho III.[3] The SAD data from both quenched and slow-cooled $YBa_2Cu_3O_{7-\delta}$ proves the existence of this phase for a wide range of annealing temperatures; these results are in agreement with the predictions of De Fontaine *et al.*[3,4] The lack of either APB's or Ortho III domains in the Monte Carlo simulations of Poulsen *et al.*[5] is incompatible with these experimental results.

To summarize, we produced quenched samples of $YBa_2Cu_3O_{7-\delta}$ that show a nearly linear T_c dependence on δ; slow-cooled specimens usually display a double-plateau structure. We studied the oxygen ordering of these quenched specimens using SAD in a TEM and compared these results to those of Beyers *et al.* on slow-cooled samples. The observed diffuse scattering features proved that there exist significant oxygen-ordering differences between the quenched and slow-cooled samples. We concluded that oxygen ordering has a strong effect on T_c. Finally, the experimental measurements were compared with a new oxygen-ordering model in which the average APD size is the only adjustable parameter. This model fit both our own experimental measurements and those of Beyers *et al.* to within measurement error.

We acknowledge gratefully many insightful conversations with Tom Shaw. This research was partially supported by DARPA under Contract No. N00014-89-C-0112.

[1]R. Beyers, B. T. Ahn, G. Gorman, V. Y. Lee, S. S. P. Parkin, M. L. Ramirez, K. P. Roche, J. E. Vazquez, T. M. Gur, and R. A. Huggins, Nature (London) **340**, 619 (1989).

[2]A. G. Khachaturyan and J. W. Morris, Jr., Phys. Rev. Lett. **64**, 76 (1990).

[3]D. de Fontaine, G. Ceder, and M. Asta, Nature (London) **343**, 544 (1990).

[4]C. Ceder, M. Asta, and D. de Fontaine, Physica C **177**, 106 (1991).

[5]H. F. Poulsen, N. H. Andersen, J.V. Anderson, H. Bohr, and O. G. Mouritsen, Nature (London) **349**, 594 (1991).

[6]Joachim Stolze, Phys. Rev. Lett. **64**, 970 (1990).

[7]R. J. Cava, A. W. Hewat, E. A. Hewat, B. Batlogg, M. Marezio, K. M. Rabe, J. J. Krajewski, W. F. Pech, Jr., and L. W. Rupp, Jr., Physica C **165**, 419 (1990).

[8]J. D. Jorgensen, Shiyou Pei, P. Lightfoot, Hao Shi, A. P. Paulikas, and B. W. Veal, Physica C **167**, 571 (1990).

[9]G. Van Tendeloo and S. Amelinckx, J. Less-Common Met. **164**, 92 (1990).

[10]B. Raveau, C. Michel, M. Hervieu, D. Groult, and J. Provost, J. Solid State Chem. **85**, 181 (1990).

[11]M. Hervieu, B. Domenges, B. Raveau, M. Post, W. R. McKinnon, and J. M. Tarascon, Mat. Lett. **8**, 73 (1989).

[12]G. Van Tendeloo, T. Krekels, J Reyes-Gasga, J. Van Landuyt, S. Amelinckx, W. H. M. Bruggink, and H. Verweij, Physica C **162**, 945 (1989).

[13]R. J. Cava, B. Batlogg, C. H. Chen, E. A. Rietman, S. M. Zahurak, and D. Werder, Phys. Rev. B **36**, 5719 (1987).

[14]K. Salama, V. Selvamanickam, L. Gao, and K. Sun, Appl. Phys. Lett. **54**, 2352 (1989).

[15]T. B. Lindemer, J. F. Hunley, J. E. Gates, A. L. Sutton, Jr., J. Brynstad, and C. R. Hubbard, J. Am. Ceram. Soc. **72**, 1775 (1989).

[16]M. Däumling, L. E. Levine, and T. M. Shaw, Adv. Cryogen. Eng. Mater. (to be published).

[17]C. Mangung, J. T. S. Irvine, and A. R. West, Physica C **168**, 346 (1990).

[18]R. Beyers (private communication).

[19]J. Zaanen, A. T. Paxton, O. Jepson, and O. K. Anderson, Phys. Rev. Lett. **60**, 2685 (1988).